Eur. Phys. J. B **1**, 47-56 (1998)

THE EUROPEAN PHYSICAL JOURNAL B

Competition in low ordered smectics between incommensurate phases S_{ic} and two-dimensional modulated ones for dimesogenic compounds

F. Hardouin[1,a], M.F. Achard[1], J.-I. Jin[2], Y.-K. Yun[2], and S.-J. Chung[2]

[1] Centre de Recherche Paul Pascal, Université Bordeaux I, avenue A. Schweitzer, 33600 Pessac, France
[2] Department of Chemistry, College of Sciences, Korea University, Seoul 136-701, Korea

Received: 26 June 1997 / Revised: 7 October 1997 / Accepted: 29 October 1997

Abstract. Systematic physical chemistry studies are in progress concerning the occurrence of incommensurate low ordered smectic phases (S_{ic}) in non-symmetric dimesogens varying molecular parameters from the standard compound KI-5. In the present study, the selected molecules possess the same spacer length and the same cholesteryl unit. By means of X-ray diffraction on orientated samples, commensurate phases, incommensurate fluid smectics and two-dimensional ones are clearly evidenced depending both on temperature and molecular parameters. So these dimesogenic compounds respond to the frustration connected to the competition between two incommensurate lengths with the formation either of an incommensurate phase S_{ic} or of a two-dimensional modulated phase. A new topology in a phase diagram results from this competition in a binary system composed of two homologous dimesogens.

PACS. 61.30.-v Liquid crystals – 61.30.Eb Experimental determinations of smectic, nematic, cholesteric, and other structures – 64.70.Md Transitions in liquid crystals

1 Introduction

As part of polar mesogens study, the model of "frustrated smectics" [1–6] was able to explain the great number of low ordered smectic phases experimentally discovered [7] and also predicted the existence of incommensurate smectic phases. This mean-field theory is based on the competition of two incommensurate lengths, namely the length of the polar molecule and the length of a pair formed by dipolar association. The impossibility to satisfy simultaneously contradictory tendencies is solved in different ways: lock-in of the two periods (bilayer S_{A2}), condensation of one period with the coexistence a non condensed second period giving incommensurate fluctuations [8,9], escape from the incommensurability by forming two-dimensional modulated phases in which the two density modulations do not remain collinear (antiphase $S_{\tilde{A}}$ [10] or ribbon phase $S_{\tilde{c}}$ [11]). Finally incommensurate smectic A phases, in which the two competing periodicities coexist at long range order along the same direction, are prognosticated. Experimentally speaking, the existence of incommensurate S_{Aic} [12–14] or S_E [15,16] has been questioned in polar systems and only incommensurate crystal-B phase has been clearly evidenced so far [17].

Note that the molecular origin of the two competing lengths is not necessarily those of polar mesogens [18–20]: thus, the potentiality of two smectic modulations to exist in other liquid crystalline systems is suggested. In particular in non-symmetric dimesogens, constituted of two chemically different mesogenic groups linked together by a flexible spacer, which belong to a new class of liquid crystals extensively studied at this time [20–41], two smectic modulations have been observed: one corresponds to a layer spacing approximately half the molecular length revealing a so called "intercalated structure" and the other to a layer spacing close to (or greater than) the dimesogen length [30]. By comparison to polar smectics, the smectic layering associated to average monomer arrangement and to the whole dimesogen length are respectively analogous to a monolayer smectic A1 and to a bilayer S_{A2}. Note that the driving forces which control a monomeric packing or a dimeric one are at the present time not clear. Nevertheless, the condensation of one or the other of these smectic modulations and their possible coexistence appear closely related to the length of the flexible spacer linking the two mesogenic moieties: in new dimesogenic molecules composed of two very different mesogenic units — a cholesteryl one and a classical two aromatic rings mesogen — connected through a central paraffinic flexible spacer [20,32], the smectic layering is connected to the "dimer" length for short spacers while longer spacers homologues correspond to a "monomer-like arrangement". In these series, we reported the existence of incommensurate low ordered smectic phase S_{ic} for specific intermediate spacer length [20].

[a] e-mail: f.hardouin@presidence-bx1.u-bordeaux.fr

Starting from this first observation of S_{ic} phase in the following dimesogen (KI-5 for short): the question of

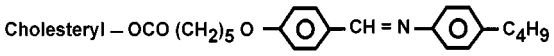

the dependence of the formation of incommensurate fluid smectic phases upon molecular parameters is raised and the thermal and structural investigations on several homologues of KI-5 can solve partially this problem.
In this study, we keep the same cholesteryl part and the same spacer length with five methylene groups as in KI-5 and two molecular parameters connected to the other mesogen are modified, namely the nature of the terminal chain ("KII-5" compound) and the kind of linking group

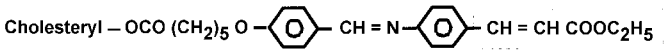

between the two aromatic rings ("KI-5A" compound):

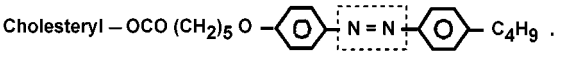

2 Synthesis

Synthesis of N-[4-(5-(cholesteryloxycarbonyl)pentyloxy) benzylidene] (4-(ethoxy-carbonylvinylene)aniline: KII-5

Ethyl 4-aminocinamate [42] (7.0 g; 3.36×10^{-2} mol) and 4.5 g (3.68×10^{-2} mol) of 4-hydroxybenzaldehyde were dissolved in 200 mL of benzene. The mixture was refluxed for 6 hours under a dry nitrogen atmosphere. And then benzene was distilled out and the residue recrystallized from methanol to produce 7.7 g (2.57; 10^{-2} mol; 70%) of N-(4-hydroxybenzylidene 4-(ethoxycarbonylvinylene)-aniline.

The melting point of the product was 184 °C. The structure was confirmed by elemental and IR- and NMR-spectroscopic analyses. N-(4-hydroxybenzylidene)4-(ethoxycarbonylvinylene)aniline (2.5 g; 8.47 mmol) above prepared was dissolved in 100 mL of DMF containing a small amount of molecular sieve (4 Å). To this solution were added 0.45 g (4.24 mmol) of sodium carbonate and 4.6 g (8.2 mmol) of cholesteryl 6-bromohexanoate [20]. The mixture was stirred at 100 °C for 12 hours under a dry nitrogen atmosphere. The whole reaction mixture was cooled down and the insoluble portion was collected on a filter followed by washing with DMF. The product was extracted from the solid residue using dry methylene chloride. Methylene chloride was evaporated to obtain the product, KII-5. Yield was 3.6 g (55%). The structure was confirmed by elemental and IR- and NMR-spectrocscopic analyses.

Synthesis of cholesteryl 6-[4-(4-butylphenylazo) phenoxy] hexanoate: KI-5A

4-(4-butylphenylazo)phenol [43] (4.73 g; 1.86×10^{-2} mol) was dissolved in 150 mL of N,N-dimethylformamide (DMF), to which added were sodium carbonate (4.33 g; 4.09×10^{-2} mol) and cholesteryl 6-bromohexanoate [15] (7.0 g; 1.24×10^{-2} mol). The mixture was stirred at 135 °C for 12 hours under dry nitrogen atmosphere, after which it was cooled down to room temperature. The precipitate was collected on a filter and washed with distilled water, methanol and acetone. Yield was 6.7 g (73%). The structure of the product was confirmed by elemental and IR- and NMR-spectroscopic analyses.

3 Experiment

An initial identification of the liquid crystalline phases was carried out using thermal optical microscopy (Leitz microscope equipped with a Mettler FP52 hot stage). Observations were systematically made either without surface treatment of the substrate or with rubbed polyimide aligning agent resulting in a planar texture. The temperature range of each phase was detected *via* differential scanning calorimetry (Perkin Elmer DSC7). The identifications of the phase sequences were carried out using the characteristic features of the X-ray patterns.

In order to study well aligned samples by X-ray analysis, the following procedure was used: two thin glass plates (< 50 μm, obtained by controlled attack of glass slide by hydrofluoric acid) were coated with polyimide and unidirectionnaly rubbed and adjusted in antiparallel configuration with a spacer of 25 μm to form a cell. The liquid crystal was then introduced by capillarity at high temperature and subjected to mechanical stress perpendicular to the rubbing direction to improve the alignment. The quality of the alignment is controlled under microscope.

The X-ray scattering experiments were carried on a 18 kW rotating anode X-ray source (Rigaku-200) with use of Ge(111) crystal as monochromator to select the $CuK_{\alpha 1}$ radiation and a three slit collimation scheme. The scattered radiation was collected on a two-dimensional detector (Imaging Plate system from Mar Research, Hamburg).

We define q_z as the component of the scattering wavevector parallel to the rubbing direction and q_x as the component perpendicular. The magnitude of the q wave vector is given by $q = 4\pi/\lambda \sin\Theta = 2\pi/d$, d is a layer parameter. The scattered resolution in terms of half width at half maximum (HWHM) was $\Delta q_z = 4 \times 10^{-3}$ Å^{-1} in the longitudinal direction and $\Delta q_x = 2 \times 10^{-3}$ Å^{-1} in the transverse direction with a sample to detector distance of 830 mm. In some cases, measurements were also done in a lower resolution configuration characterized by Δq_z and $\Delta q_x = 10^{-2}$ Å^{-1}.
The samples were placed in an oven, providing a temperature control of 0.1 K.

4 Results and discussion

4.1 Occurrence of an S_{Aic} in the KII-5 compound

As shown in the formula, the KII-5 compound is an homologue of KI-5 with a longer and more rigid extremity [32] and its behavior is discussed in detail below. The complementary techniques allow to determine the following phase sequence:

$$\text{crystal} \xrightarrow{139^\circ\text{C}} S_{LT} \xrightarrow{140^\circ\text{C}} S_{HT} \xrightarrow{206^\circ\text{C}} N^* \xrightarrow{238^\circ\text{C}} I$$

where S_{LT} and S_{HT} denote two smectic phases. Although this weakly first order S_{LT}–S_{HT} transition (ΔH = 78 J mol^{-1}) is seen by differential scanning calorimetry, optical microscopy do not show any difference in textures of the two smectic phases.

In the whole smectic range, the intensity profiles of the X-ray pattern in the wide scattering angles region show broad diffuse band (Fig. 1a). Thus, the two smectic phases of KII-5 have to be referred as fluid smectic phases (liquid like short range order within the layers). The liquid like peaks are centered around $q_x = 1.25$ Å^{-1} corresponding to average intermolecular distance of 5 Å in the smectic planes. Figures 1b and 1c show the low angle region X-ray patterns of an orientated sample of KII-5 in the two smectic phases.

The pattern of the high temperature smectic phase S_{HT} (Fig. 1b) is characterized by one resolution limited peak at $q_3 = 0.302$ Å$^{-1} = 2\pi/20.8$ Å. This phase is labelled S_{q_3}. We can note that the ratio of the layer spacing to the estimated all-trans molecular length (50 Å) is unusually small (0.4) by comparison to the intercalated structure of other non symmetric dimesogens [21,26,30]. Decreasing temperature in this S_{HT} phase, a diffuse peak centered at an incommensurate wavenumber q_1 with regard to the scattering vector q_3 is observed: $q_1 = 2\pi/L'$ varying from 0.130 to 0.122 Å^{-1}. By reference to polar smectics studies, this type of structure could be considered analogous to a "monolayer S_{A1} phase" in which an S_{Ad} modulation coexists at short range order thus forming something like incommensurate fluctuations [9].

At temperatures lower than 140 °C, the orientated pattern of the low temperature smectic phase S_{LT} (Fig. 1c) clearly demonstrates the simultaneous existence of three resolution limited peaks. The corresponding diffraction vectors q_1, q_2 and q_3 are collinear. As shown on the corresponding intensity profile (Fig. 2), the intensity of q_2 is very weak. But although reduced in intensity by a factor 100 by comparison to q_1, this peak is undoubtly detected. The existence of these three collinear wave vectors reflect the occurrence of a genuine incommensurate smectic S_{Aic} phase with two underlying incommensurate smectic modulations at q_1 and q_3. The small peak at q_2 corresponds to a satellite which is the signature of a superlattice for this incommensurate smectic phase. The ratio of the two periods q_3/q_1 is an irrational number clearly larger than 2. As shown in Figure 3, the wavevector q_1 evolves continuously from 0.130 to 0.119 Å^{-1} while the q_3 wavevector remains located at constant value $q_3 = 0.302$ Å^{-1}.

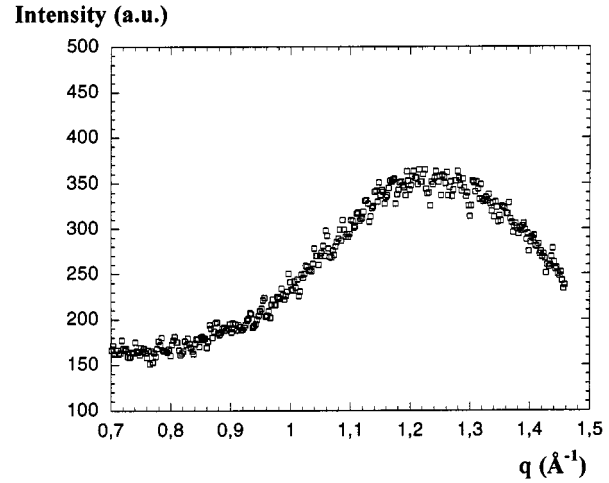

(a)

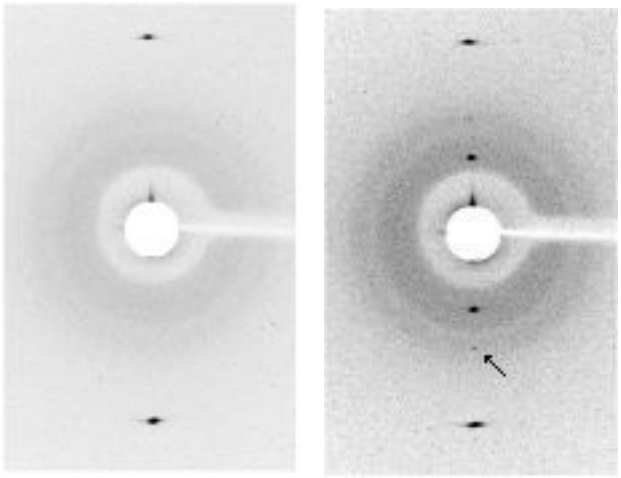

(b) (c)

Fig. 1. X-ray data of KII-5: (a) intensity profile at wide angles at 135 °C; (b) and (c) X-ray patterns of an orientated sample: (b) at $T = 160$ °C corresponding to the high temperature smectic phase; (c) at $T = 135$ °C corresponding to the low temperature smectic (the arrow points the q_2 spot).

So this incommensurate structure is characterized by the superposition of two periodicities, with a ratio of the periods not fixed and depending continuously of temperature: $2.32 < q_3/q_1 < 2.54$. The incommensurability parameter $\varepsilon_1 = (q_3 - 2q_1)/q_3$ measures the degree of mistmach between $2q_1$ and q_3 and this S_{Aic} of KII-5 corresponds to large incommensurability ($\varepsilon_1 = 0.21$). This phase extends in a supercooled state down to 124 °C where crystallization is observed (Fig. 3) with the occurrence of several sharp reflections at wide angles and a commensurate lamellar organization with $q_1 = 0.105$ Å^{-1} and several harmonics $2q_1$, $3q_1$ ... Note that in the S_{Aic}, the three

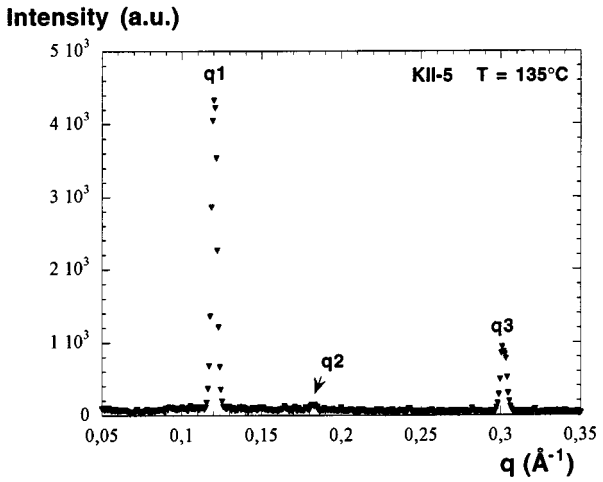

Fig. 2. Intensity profile corresponding to the pattern of Figure 1c.

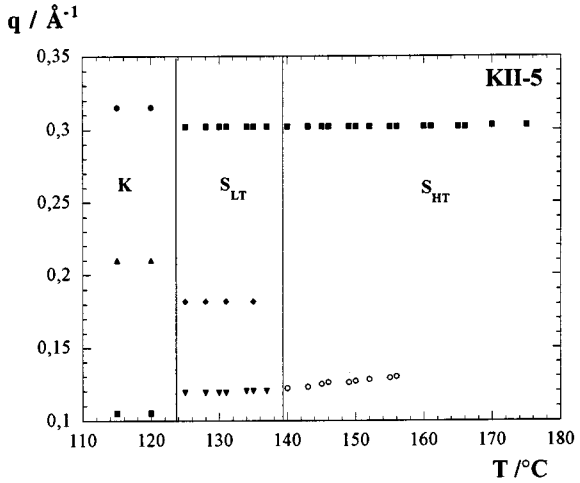

Fig. 3. Magnitudes of the q_1, q_2, q_3 diffraction vectors as a function of temperature. Filled symbols indicate resolution limited peaks. The open circles correspond to diffuse maxima centered at q_1 (since q_1 is not condensed in the S_{HT} phase, see text).

wavevectors comply with the additivity condition initially set for biaxial lockins [2,3], $q_3 = q_1 + q_2$: at 135 °C, $q_1 = 0.120$ Å$^{-1} = 2\pi/52.3$ Å, $q_2 = 0.182$ Å^{-1} and $q_3 = 0.302$ Å$^{-1} = 2\pi/20.8$ Å. So this condition seems also satisfied in an incommensurate S_{Aic} phase in which the three vectors are collinear.

We recall that in the Prost-Barois phenomenological theory, two types of incommensurate smectic A phases are predicted in polar systems depending on the strength of the coupling between the two order parameters [6]: a weakly coupled incommensurate phase where two penetrating smectic modulations coexist independently of each other, with periodicities of molecular length and of overlapping dimer-like associations; and a strongly coupled incommensurate soliton phase where regions with two independent wave vectors separate regions in which the two modulations are phase locked (Fig. 4) due to the fact that

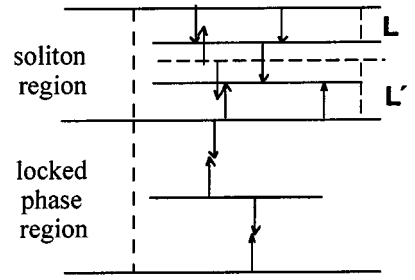

Fig. 4. Real space representation of the incommensurate soliton phase corresponding to a strong coupling regime.

the polar molecules form dimer-like arrangements with no overlap or with partial overlap.

In the case of KII-5, the third reflection q_2 is the signature of an incommensurate soliton smectic structure. At a microscopic level, the schematic representation corresponding to the predicted incommensurate soliton phase for polar systems has to be adapted to dimesogenic compounds and an interesting question is how these nonsymmetric dimesogens are arranged to form such unusual structure. X-ray results give some indications on the molecular packing: first the smectic periodicity connected to q_1 is larger than the estimated molecular length obtained from molecular stereomodels, suggesting associated dimesogens. In addition, preliminary molecular mechanics calculations show an energetically favourable antiparallel organization. Second, the small periodicity connected to q_3 appears quasi independent of the chemical formula of cholesteryl dimesogens varying either the spacer length [32] or the aromatic mesogen [32]. Thus this small periodicity (≈ 21 Å) seems to be imposed by the cholesteryl moiety while the second mesogenic part adapt to this layering size and this smectic order is presumably stabilized by the mixed mesogenic group interactions. The formation of this enforced periodicity is required to develop the incommensurate structure. Nevertheless, a complete microscopic description of the arrangement of the dimesogens remains an unresolved matter and theoretical computations (molecular mechanics and dynamics) are expected to solve this challenge in a realistic way.

At last, referring again to the theory, we can remind that the importance of the coupling between the two order parameters depends on the ratio of the two corresponding lengths [6]. As just seen, q_3/q_1 is about 2.54 for KII-5. In the case of KI-5, the two wave vectors are closer ($q_3/q_1 \approx 2.1$) and thus the coupling is stronger. In this sense it is interesting to study now the evolution of the incommensurability through the "KII-5/ KI-5" binary phase diagram.

4.2 Evolution of the S_{Aic} through the KII-5/KI-5 binary phase diagram

For a large part of the phase diagram ($0 < x < 0.800$, where x is the molar fraction of KI-5 in a mixture) the $S_{q_3}-S_{Aic}$ smectic sequence is observed as for the pure

KII-5: the S_{q_3} phase exhibits two incommensurate lengths, one is condensed into a long range layer structure (q_3) and the other (q_1) persists at short range order resulting in incommensurate fluctuations. The signature of the incommensurate S_{Aic} phase is always given by the existence of three collinear wave vectors (Fig. 5) and as in the case of KII-5, the law of conservation of vectors $q_3 = q_1 + q_2$ is satisfied in the S_{Aic} phase whatever the composition.

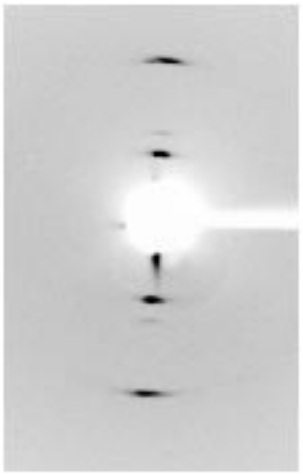

Fig. 5. X-ray pattern of an orientated mixture ($x = 0.760$) at $T = 100$ °C in the S_{Aic} phase.

Table 1 summarizes the diffraction data for different mixtures. One can first note the linear shift down of the incommensurability parameter ε_1 increasing the proportion of KI-5 in the mixtures, traducing a greater coupling between the two order parameters. Correlatively, the q_2 satellite becomes more intense (Fig. 5). As listed in Table 1 the regular evolution of q_3/q_1 *versus* composition in the incommensurate S_{Aic} phase is correlated to the modification of the wave vector q_1 since the magnitude of the wavevetor q_3 is quasi independent of the composition and of the nature (S_{q_3} or S_{Aic}) of the phase. Indeed, the smaller periodicity remains fixed (20.8 Å for KII-5 and 20.2 Å for $x = 0.76$) while, at the opposite, the larger periodicity takes an average value between the lengths of the two dimesogens varying the composition of the KII-5/KI-5 mixtures (52.3 Å for KII-5 and 45.8 Å for $x = 0.76$). So the incommensurate structure changes and adapts itself to the presence of two different mesogenic entities. But approaching the pure KI-5, some unexpected features are observed on the orientated patterns of the S_{q_3} phase: the incommensurate fluctuations at $\langle q_1 \rangle$ evolve towards off axis suggesting the vicinity at low temperature of a two-dimensional modulated smectic phase near the incommensurate S_{Aic} phase. Thus we focus now on the pure KI-5 then on mixtures with high proportions of KI-5 ($x > 0.800$).

Table 1. X-ray data for the KII-5-KI-5 binary system. For the S_{Aic} phases, data are recorded 5 degrees below the S_{q_3}−S_{Aic} transition temperature.

Phase	S_{q_3}	S_{Aic}				
x_{KI-5}	q_3(Å^{-1})	q_1(Å^{-1})	q_2(Å^{-1})	q_3(Å^{-1})	q_3/q_1	ε_1
0	0.302	0.120	0.182	0.302	2.52	0.205
0.157	0.303	0.123	0.180	0.303	2.46	0.188
0.260	0.304	0.125	0.179	0.304	2.43	0.178
0.408	0.307	0.129	0.178	0.307	2.38	0.160
0.544	0.309	0.132	0.177	0.309	2.34	0.146
0.662	0.310	0.134	0.176	0.310	2.31	0.132
0.760	0.311	0.137	0.174	0.311	2.27	0.119

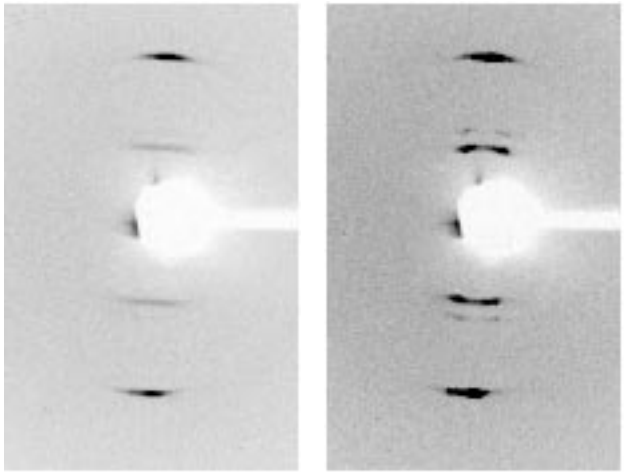

(a) (b)

Fig. 6. X-ray pattern of an orientated KI-5 sample: (a) at $T = 110$ °C, $q_3 = 0.313$ Å^{-1} and $\langle q_1 \rangle = 0.144$ Å^{-1}. Note that the incommensurate fluctuations $\langle q_1 \rangle$ correspond to a rather large correlation length $\xi_z = 200$ Å; (b) at $T = 95$ °C, $q_3 = 0.313$ Å^{-1}, $q_1 = 0.142$ Å^{-1}, and $q_2 = 0.178$ Å^{-1}. In the limit of our experimental accuracy, the three wave vectors satisfy the relation $q_3 = q_{1z} + q_{2z}$.

4.3 Competition between incommensurate and two-dimensional smectic phases

4.3.1 Occurrence of a two-dimensional smectic in the pure KI-5

A well orientated pattern of the S_{q_3} phase of KI-5 (Fig. 6a) is characterized by a resolution limited peak centered on the z axis at q_3 and by strong incommensurate fluctuations at q_1 (and weaker ones at q_2) with a clear lateral extension along q_x. This tendency to a two-dimensional phase is confirmed at lower temperature since a phase transition is observed at 97 °C corresponding to an extremely weak enthalpy change ($\Delta H = 15$ J mol^{-1}). The pattern of this low temperature smectic phase (Fig. 6b) shows

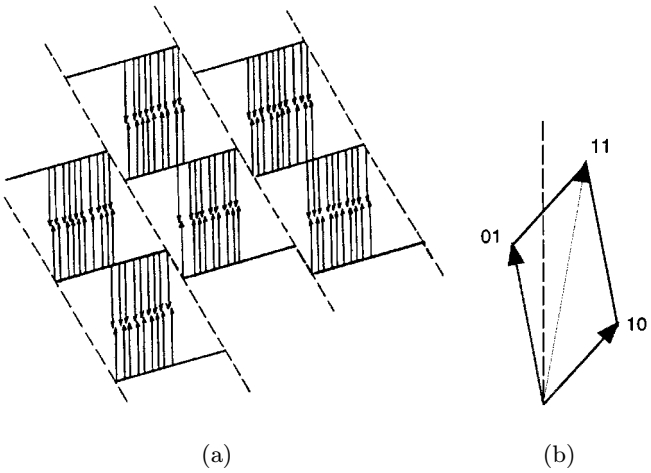

Fig. 7. (a) Real space representation of the ribbon phase $S_{\tilde{c}}$ for polar systems. (b) Possible matching of the wave vectors in a two-dimensional vector space.

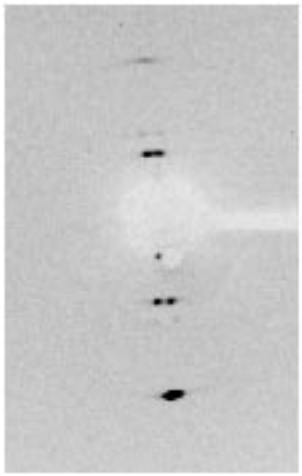

Fig. 8. X-ray pattern for KII-5-0.85 KI-5 mixture at 90 °C.

resolution limited peaks at q_1, q_2 and q_3 which are no longer collinear. The fluid local order is kept in this temperature range [20]. The simplest way to index this phase is a ribbon phase $S_{\tilde{c}}$ ([11], Fig. 7) even if the pattern appears unusually symmetric: in the limit of our experimental accuracy, q_3 remains centered on the z axis while the sets of reflections connected to q_1 and q_2 are symmetrically disposed out of the z axis with comparable angular shift (12°). Thus the z axis is a symmetry axis of the reciprocal lattice and this could be explained in an $S_{\tilde{c}}$ if the conditions of preparation of the sample fix the orientation of the normal to the planes and not of the long axes of the molecules. One can also note that the intensities of the reflections corresponding to q_1 and q_3 are of the same order of magnitude while the q_2 spot is 10 times less intense: usually, in a "classical $S_{\tilde{c}}$" the intensities of the 01 (q_2) and 11 (q_3) peaks are comparable while the intensity of the 10 reflex (q_1) is very low [11,44,45]. In addition, as later mentioned, this phase indexed $S_{\tilde{c}}$ appears very near to a real incommensurate S_{Aic} and can exhibit the same local order.

So referring to these new data, the following phase assignment is given for KI-5:

$$\text{crystal} \xrightarrow{85^\circ C} S_{\tilde{c}} \xrightarrow{97^\circ C} S_{q_3} \xrightarrow{141^\circ C} S_{ic} \xrightarrow{146^\circ C} S_{c^*LT} \xrightarrow{152^\circ C} S_{c^*HT} \xrightarrow{164^\circ C} TGB \xrightarrow{168^\circ C} N^* \xrightarrow{192^\circ C} I.$$

Note that this complex sequence includes a small incommensurate S_{ic}[1] phase characterized by three collinear resolution limited peaks $q_1 = 0.149$ Å^{-1}, $q_2 = 0.164$ Å^{-1} and $q_3 = 0.313$ Å^{-1}. It corresponds to a small incommensurability parameter $\varepsilon_1 = 0.04$, *e.g.* to a strong coupling. So the competition between incommensurate and two-dimensional phases is peculiarly obvious in the pure KI-5 since both phases exist in its mesomorphic sequence. Nevertheless, S_{ic} and $S_{\tilde{c}}$ phases remain separated by a large S_{q_3} domain. At this step, let us focus again on the KII-5/KI-5 diagram in the region of high concentration for KI-5.

4.3.2 A new $S_{Aic}-S_{\tilde{c}}-S_{q_3}$ topology in the KII-5/KI-5 binary diagram

As expected, the competition between an incommensurate phase S_{Aic} and a two-dimensional $S_{\tilde{c}}$ is directly observable as a region of the KII-5/KI-5 diagram near KI-5. Varying the composition, from pure KI-5 in the $S_{\tilde{c}}$ phase, the off axis spots q_1 and q_2 (Fig. 6b for KI-5) go towards the z axis (Fig. 8 for $x = 0.85$) and become collinear with q_3 when $x < 0.800$ (see Fig. 5). Figure 9 shows the corresponding X-ray intensity profiles as a function of q_x at constant q_{1z}. In the real space, the corresponding wave length $2\pi/q_x$ which gives the magnitude of the lateral modulation strongly increases from 180 Å for KI-5 to 1050 Å for $x = 0.85$ and diverges approaching $x = 0.800$ giving rises to the incommensurate S_{Aic}. In the same way, increasing temperature at constant composition ($x = 0.85$), the $S_{\tilde{c}}$ phase changes into a continuous process into the S_{Aic}. Clearly, high resolution X-ray studies are required for a better understanding of the incommensurate - two-dimensional phase change.

So this domain near the KI-5 of the KII-5/KI-5 diagram (Fig. 10) is characterized by three phase lines converging in a $S_{Aic}-S_{\tilde{c}}-S_{q_3}$ singular point. The transitions $S_{q_3}-S_{Aic}$ and $S_{q_3}-S_{\tilde{c}}$ are weakly first order, while the $S_{\tilde{c}}-S_{Aic}$ phase change appears second order. We can note that the competition between S_{Aic} and $S_{\tilde{c}}$ occurs when the coupling between the two order parameters is rather strong ($\varepsilon_1 \approx 0.08$). The topology of this part of the experimental phase diagram reminds the theoretical diagram proposed by Prost *et al.* [2] in the case of polar mesogens where S_{A2}, S_{Aic}, and $S_{\tilde{A}}$ were brought together. Depending on the theoretical parameters, the calculated

[1] Note that the distinction between A or C phases is not obvious since the smectic C phases correspond to small tilt angles. So we focus on the incommensurablity aspect rather than on the A or C nature of the phases.

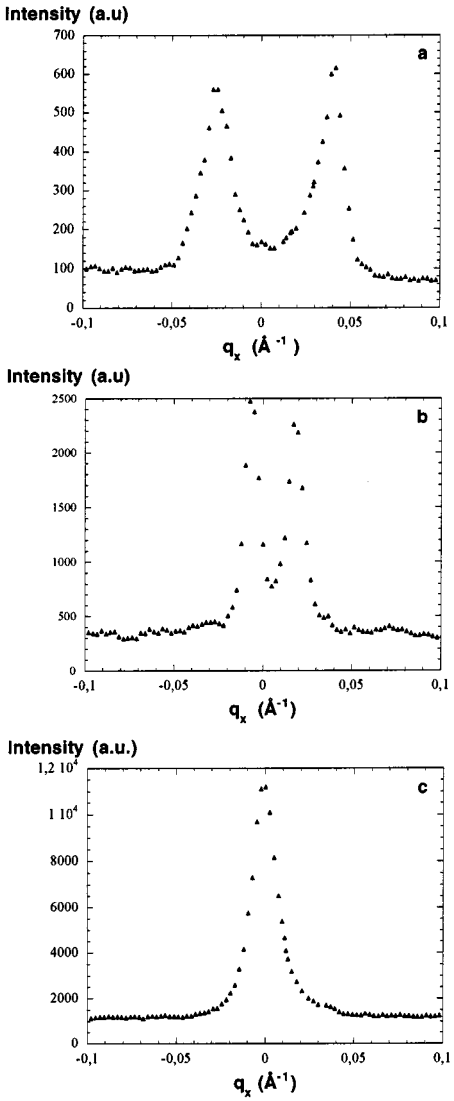

Fig. 9. X-ray intensity as a function of q_x at constant q_{1z}; (a) $S_{\tilde{c}}$ for pure KI-5 ($q_{1z} = 0.142$ Å^{-1}); (b) $S_{\tilde{c}}$ for KII-5-0.85 KI-5 mixture ($q_{1z} = 0.134$ Å^{-1}); (c) S_{Aic} for KII-5-0.76 KI-5 mixture ($q_{1z} = 0.137$ Å^{-1}) Note that similar evolution is observed for q_2 spots.

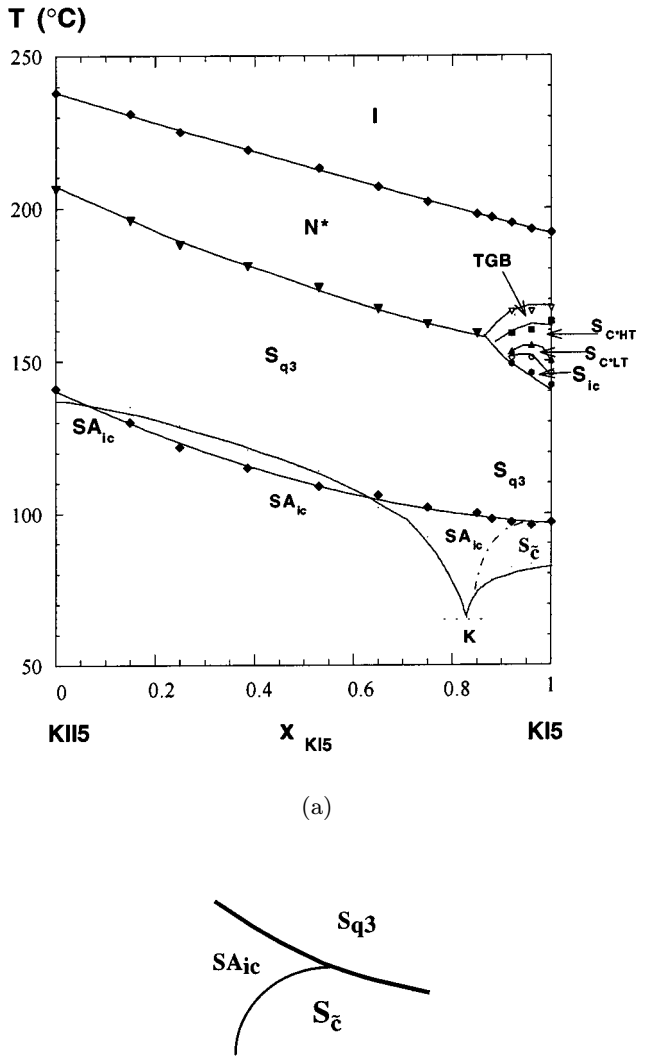

(a)

(b)

Fig. 10. (a) Isobaric temperature-concentration phase diagram between the two homologous dimesogenic compounds: KII-5 (left) and KI-5 (right). Note that the high temperature smectic phases of KI-5 (TGB, S_{c*HT}, S_{c*LT}, and S_{ic}) disappear on adding KII-5. In addition note that in a part of the diagram, the S_{Aic} is monotropic: this phase exists in a supercooled state 15−20° below the melting point, before crystallization. (b) Schematic representation of the new S_{Aic}−$S_{\tilde{c}}$ − S_{q_3} topology.

phase diagram shows a commensurate S_{A2} phase, an incommensurate phase S_{Aic} and an antiphase $S_{\tilde{A}}$ with $q_x \neq 0$ which appears as a two-dimensional escape to incommensurate phases. Using the same model, Wang and Lubensky predict that the competition between incommensurate phase and antiphase may be directly observable as a region of coexisting incommensurate and $S_{\tilde{A}}$ fluctuations [46]. Experimentally, high resolution X-ray analysis underlines the complicated behavior of the polar systems in the vicinity of S_{A1}−$S_{\tilde{c}}$ [44] and S_{A1}−$S_{\tilde{A}}$ [9,47] transitions. For example near the S_{A1}−$S_{\tilde{A}}$ transition, Safinya *et al.* showed an intermediate region of coexisting incommensurate fluctuations with large incommensurablity and $S_{\tilde{c}}$ fluctuations [47] which strongly supports the Prost-Barois hypothesis. Lobko *et al.* [45] confirm the theoretical description of $S_{\tilde{c}}$ phase as a two-dimensional escape from incommensurability in the case of strong coupling between the two incommensurate density modulations and in this way, our experimental results closely agree with the phenomenological models initially introduced to describe the polar systems.

These results on KII-5 and KI-5 show that the systems hesitate between commensurate, incommensurate and two-dimensional fluid smectics depending both on temperature and molecular composition. At the molecular level, we have already mentioned the fundamental role

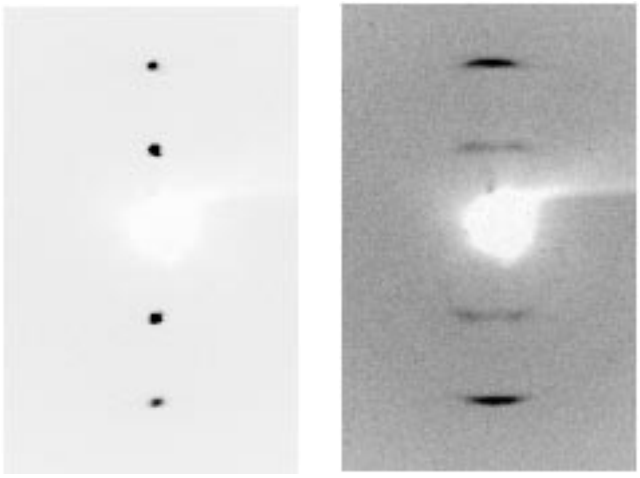

(a) (b)

Fig. 11. X-ray patterns of orientated sample of KI-5A: (a) in the high temperature smectic phase S_{HT} at 150 °C; (b) in the low temperature smectic phase at 135 °C. Note that the diffracted intensity is reduced by a factor 20 in this S_{LT} phase.

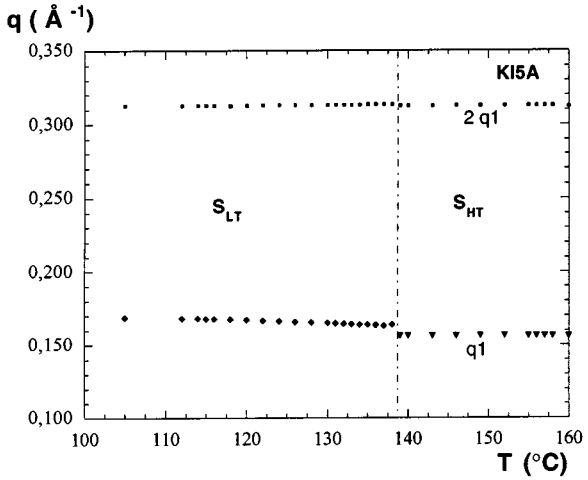

Fig. 12. Thermal evolution of the wave vectors for the KI-5A compound.

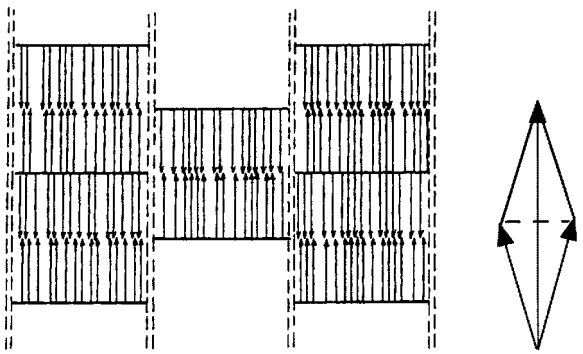

(a) (b)

Fig. 13. (a) Schematic representation of a $S_{\tilde{A}}$ antiphase for polar systems. (b) Commensurate lockin of the wave vectors n a two-dimensional vector space.

of the spacer length [32] and here we stress that the change of the terminal extremity strongly influences the polymorphism and the structural characteristics in these cholesteryl dimesogens. We will now focus our interest on another molecular parameter, the nature of the linking group between the two aromatic rings. In order to explore this way, we select the KI-5A, homologous compound of KI-5, which possesses an azo group instead of the imino one.

4.4 Occurrence of another two-dimensional smectic in the KI-5A homologous: a smectic antiphase $S_{\tilde{A}}$

The complementary techniques of characterization allow to determine a simplest phase sequence for KI-5A than for the reference compound KI-5:

$$\text{crystal} \xrightarrow{113^\circ\text{C}} S_{LT} \xrightarrow{137^\circ\text{C}} S_{HT} \xrightarrow{160^\circ\text{C}} \text{TGB} \xrightarrow{163^\circ\text{C}} N^* \xrightarrow{194^\circ\text{C}} I$$

where S_{LT} and S_{HT} indicate two low ordered smectic phases.

The high temperature smectic S_{HT} exhibits a resolution limited peak corresponding to a large periodicity $q_1 = 0.156$ Å$^{-1} = 2\pi/40.2$ Å, with another intense spot of the first harmonic at $2q_1 = 0.312$ Å^{-1} (Fig. 11a). As shown in Figure 12, q_1 is no temperature dependent in the S_{HT} phase.

The $S_{HT}-S_{LT}$ transition is characterized by a significant enthalpy change ($\Delta H = 206$ J mol^{-1}) and by the appearance of a weakly birefringent texture on homeotropically aligned samples. From a structural point of view, the lower q spot loses its unidimensional form and splits into two spots located off the z axis at $q_1 = 0.163$ Å^{-1} (Fig. 11b). The second Bragg spot is no more the harmonic but it remains along the z axis with the same location at $q_3 = 0.312$ Å^{-1}. In the limit of our accuracy, q_3 and the projection of q_1 along the z axis are commensurate: $2q_{1z} = q_3$. This pattern is the signature of a two-dimensional rectangular centered antiphase $S_{\tilde{A}}$ ([10], Fig. 13). In the real space, the lateral modulation in the layers exhibits a large wavelength $2\pi/q_{1x} = 145$ Å which decreases as temperature decreases (110 Å at 105 °C).

Even if its chemical formula is closely related to KI-5, KI-5A does not exhibit incommensurate phase and escapes from the incommensurability by producing a two-dimensional antiphase. It is quite surprising that these chemically similar compounds significantly differ in their mesomorphic low temperature phase sequence: $S_{ic}-S_{q_3}-S_{\tilde{c}}$ for KI-5 and $S_{\tilde{A}}$ for KI-5A. As shown in Figure 14, by mixing KI-5 and KI-5A, the S_{q_3} and $S_{\tilde{c}}$ phases are observed in a large domain of concentration. The S_{q_3} phase is characterized by a resolution limited peak centered on the z axis at constant $q_3 = 0.313$ Å^{-1} and by two-dimensional fluctuations either $S_{\tilde{c}}$-like or $S_{\tilde{A}}$-like depending both on composition and temperature: a change between these two

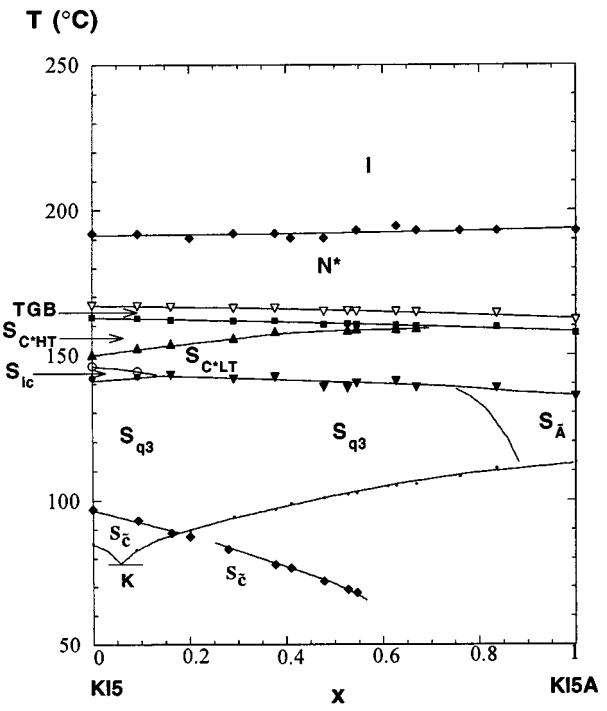

Fig. 14. Isobaric temperature-concentration phase diagram between the two homologous dimesogenic compounds: KI-5 (left) and KI-5A (right). As in the first diagram, the S_{ic} of KI-5 promptly disappears on adding KI-5A. Note that no enthalpy change corresponding to the $S_{q_3}-S_{\tilde{A}}$ transition has been detected so far and the $S_{q_3}-S_{\tilde{A}}$ line only suggests the transition.

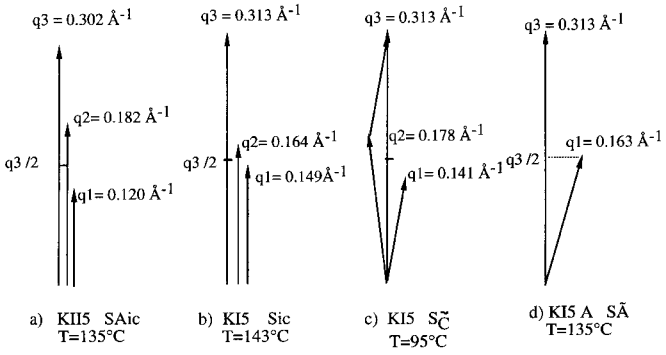

Fig. 15. Incommensurates smectic phases S_{ic} or two-dimensional $S_{\tilde{c}}$ or $S_{\tilde{A}}$ phases in the KII-5, KI-5 and KI-5A dimesogenic compounds. Note the small angular shift in (12°) and in $S_{\tilde{A}}$ (16°) by comparison with results of references [35,39,41].

regimes is detected in the 0.5−0.8 concentration range. In the $S_{\tilde{c}}$ phase, the magnitudes of the wave vectors are weakly affected by the composition and the wavelength $2\pi/q_{1x}$ relative to the in-layer modulation remains quasi constant (≈ 150 Å) varying the proportion of KI-5A. So, contrary to the KII-5-KI-5 system, the two-dimensional $S_{\tilde{c}}$ phase of KI-5 has no tendency to transform into an incommensurate phase on adding the azo derivative KI-5A. In addition, no connection is observed in the KI-5/KI-5A phase diagram between the $S_{\tilde{c}}$ and $S_{\tilde{A}}$ domains.

5 Concluding remarks

In conclusion, this work shows that the occurrence of incommensurate fluid smectic phases is bound by strict molecular conditions and at the present time remains an exception. Indeed, even if two-dimensional smectics have been already reported in dimesogenic compounds (modulated hexatic $S_{\tilde{c}}$ in symmetric dimers [35], or $S_{\tilde{A}}$ respectively in chiral [39] and polar [41] non symmetric dimesogens), incommensurate fluid smectics have never been detected. So, despite the great number of liquid crystalline materials, polar or non polar mesogens or more recently dimesogens, KI-5 and KII-5 are the only two examples exhibiting such incommensurate fluid S_{ic} phases. In addition, these dimesogens respond to the frustration connected to the competition in the low ordered smectic states between two different layer spacings with the formation either of incommensurate structures or, as in polar systems, of two-dimensional lattices. In this sense, the KII-5/ KI-5 diagram allows for the first time to bring together incommensurate smectic phase and two-dimensional one.

By comparison with other families of dimesogens, the prime novelty of the KI-5 and KII-5 compounds originates from the unusual mesogenic moiety constituted by the cholesteryl part. It is obvious that this group plays a specific role: its non aromatic nature connected to its planar shape and its strong ability to interact favourably with the aliphatic chains as well as with the aromatic rings allow a peculiar local arrangement which dictates one periodicity. Indeed, the condensed wave vector q_3 keeps a quasi constant value for the three dimesogenic compounds under study: $q_3 = 2\pi/21$ Å. From molecular models, this length corresponds to the cholesteryl moiety including the COO group of the spacer. In addition, note that this periodicity $2\pi/q_3$ exists in the whole temperature range: q_3 corresponds to the harmonic of the q_1 wave vector in commensurate phases, as fundamental wavevector in the S_{q_3} domain or as one of the coexisting wavevectors in incommensurate or in two-dimensional phases. Thus the three dimesogenic compounds essentially differ by the other periodicity, $2\pi/q_1$ which, depending on the phase, exists as long range smectic modulations or only as fluctuations. More specifically, the major difference originates from the value of q_1 by comparison to q_3: for KII-5 and KI-5, q_3/q_1 is larger than two, while for KI-5A, as in polar systems, this ratio is lower than two.

In the "frustrated smectics" model, Prost and Barois incorporate two types of relevant terms: firstly the elastic terms which describe modulations with preferences to order at incommensurate wavevector modulus $2\pi/q_1$ and secondly the coupling terms which favor the lockin, *e.g.* the commensurability. The smectic antiphases compromise between elastic and commensurability energies and in this sense will be often preferred to incommensurate phases since they minimize the commensurability energy and preserve the modulus $2\pi/q_1$ favoured by elastic terms.

The schematic representation of Figure 15 illustrates these different possibilities:

For KII-5, the coupling term is low ($\varepsilon_1 = 0.20$) and the elasticity of the system at 135 °C allows the occurrence of an incommensurate smectic phase.

KI-5 underlines the competition between the elastic and coupling terms varying temperature. At high temperature, the coupling term is rather strong ($\varepsilon_1 = 0.05$) but the elasticity of the system favours an incommensurate smectic. Unfortunately, a quantitative comparison with the model cannot be done since the temperature dependence of the different parameters have not been specified. At lower temperature, the compromise between elasticity and coupling gives rise to a two-dimensional $S_{\tilde{c}}$ phase.

At last, the KI-5A suggests that a ratio q_3/q_1 lower than two cannot generate an incommensurate fluid smectic phase since a commensurate lockin readily takes place through a $S_{\tilde{A}}$ antiphase.

Finally, with the strong chirality induced by the cholesteryl group, the helical structures, cholesteric, TGB and different kinds of S_c^* phases could be expected in these dimesogens. In contrast, the formation of incommensurate or modulated smectics is probably independent of molecular chirality but strongly depends on the presence of the cholesteryl group which dictates and fix one of the two layering periods. The variation of the molecular and thermal parameters leads to a modification of the other length giving rise to several exotic polymorphisms.

This collaborative research was cosponsored by the CNRS of France and the Korea Science & Engineering Foundation of Korea.

References

1. J. Prost, *Proceedings of the International Conference on one- and two-dimensional order* (Garmisch-Partenkirchen, Springer Verlag, Berlin, Heidelberg, New York, 1980), p. 125.
2. P. Barois, C. Coulon, J. Prost, J. Phys. Lett. France **42**, L-107 (1981).
3. J. Prost, P. Barois, J. Chim. Phys. **80**, 65 (1983).
4. P. Barois, J. Prost, T.C. Lubensky, J. Phys. France **46**, 391 (1985).
5. P. Barois, Phys. Rev. **A33**, 3632 (1986).
6. P. Barois, J. Pommier, J. Prost, *Solitons in Liquid Crystals*, edited by L. Lam, J. Prost (Springer-Verlag, New-York, 1992) p. 191
7. F. Hardouin, A.M. Levelut, M.F. Achard, G. Sigaud, J. Chim. Phys. **80**, 53 (1983) and references therein.
8. F. Hardouin, A.M. Levelut, G. Sigaud, J. Phys. France **42**, 71 (1981).
9. E. Fontes, P. Heiney, P. Barois, A.M. Levelut, Phys. Rev. Lett. **60**, 1138 (1988).
10. G. Sigaud, F. Hardouin, M.F. Achard, A.M. Levelut, J. Phys. France **42**, 107 (1981).
11. F. Hardouin, H.T. Nguyen, M.F. Achard, A.M. Levelut, J. Phys. Lett. France **43**, L-327 (1982).
12. S. Kumar, L. Chen, V. Surendranath, Phys. Rev. Lett. **67**, 322 (1991).
13. P. Patel, S. Kumar, Europhys. Lett. **23**, 135 (1993).
14. P. Patel, Chen Li, Kumar S., Phys. Rev. E **47**, 2643 (1993).
15. G.J. Brownsey, A.J. Leadbetter, Phys. Rev. Lett. **44**, 1608 (1980).
16. A.J. Leadbetter, P.A. Tucker, G.W. Gray, R. Tajbakhsh, Liq. Cryst. **8**, 1 (1990).
17. J.T. Mang, B. Cull, Y. Shi, P. Patel, S. Kumar, Phys. Rev. Lett. **74** 21 (1995).
18. B.I. Ostrovskii, Liq. Cryst. **14**, 131 (1993).
19. S. Diele, S. Manke, W. Weissflog, D. Demus, Liq. Cryst. **6**, 301 (1989).
20. F. Hardouin, M.F. Achard, J.-I. Jin, J.-W. Shin, Y.-K. Yun, J. Phys. II France **4**, 627 (1994).
21. J.L. Hogan, C.T. Imrie, G.R. Luckhurst, Liq. Cryst. **3**, 645 (1988).
22. A.C. Griffin, S.R. Vaidya, Liq. Cryst. **3**, 1275 (1988).
23. C.T. Imrie, Liq. Cryst. **6**, 391 (1989).
24. J.-I. Jin, H.-S. Kim, J.-W. Shin, B.Y. Chung, B.-W. Jo, Bull. Korea Chem. Soc. **11** , 209 (1990).
25. T. Ikeda, T. Miyamoto, S. Kurihara, M. Tsukada, S. Takuze, Mol. Cryst. Liq. Cryst. **182**, 357 (1990).
26. G.S. Attard, S. Garnett, C.G. Hickmann, C.G. Imrie, L. Taylor, Liq. Cryst. **7**, 495 (1990).
27. J.-I. Jin, B.Y. Chung, J.-K. Choi, B.-W. Jo, Bull. Korean Chem. Soc. **12**, 189 (1991).
28. G.S. Attard, C.T. Imrie, F.E. Karasz, Chem. Mater. **4**, 1246 (1992).
29. R.W. Date, C.T. Imrie, G.R. Luckhurst, J.M. Seddon, Liq. Cryst. **12**, 203 (1992).
30. G.S. Attard, R.W. Date, C.T. Imrie, G.R. Luckhurst, S. Roskilly, J.M. Seddon, L. Taylor, Liq. Cryst. **16**, 529 (1994).
31. A.T.M. Marcellis, A. Koudijs, E.J.R. Sudhölter, Recl. Trv. Chim. **113** , 524 (1994).
32. F. Hardouin, M.F. Achard, J.-I. Jin, Y.-K. Yun, J. Phys. II France **5**, 927 (1995).
33. A.E. Blatch, I.D. Fletcher, G.R. Luckhurst, Liq. Cryst. **6** 18 (1995).
34. I.D. Fletcher, G.R. Luckhurst, Liq. Cryst. **18**, 175 (1995).
35. R.W. Date, G.R. Luckhurst, M. Shuman, J.M. Seddon, J. Phys II France **5**, 587 (1995).
36. A.T.M. Marcellis, A. Koudijs, E.J.R. Sudhölter, Liq. Cryst. **18**, 843 (1995).
37. V. Faye, H.T. Nguyen, V. Laux, N. Isaert, Ferroelectrics **179**, 9 (1996).
38. V. Faye, P. Barois, H.T. Nguyen, V. Laux, N. Isaert, New J. Chem. **20**, 283 (1996).
39. V. Faye, A. Babeau, F. Placin, H.T. Nguyen, P. Barois, V. Laux, N. Isaert, Liq. Cryst. **21**, 485 (1996).
40. V. Faye, H.T. Nguyen, V. Laux, N. Isaert, Mol. Cryst. Liq. Cryst. **301**, 183 (1997).
41. V. Faye, H.T. Nguyen, P. Barois, J. Phys. II France **7**, 1245 (1997).
42. J.-I. Jin, C.-S. Kang, B.Y. Chung, Bull. Korean. Chem. Soc. **11**, 245 (1990).
43. E.D. Bergmann, S. Nerkovic, R. Ikan, J. Amer. Chem. Soc. **78**, 6037 (1956).
44. E. Fontes, P.A. Heiney, J.L. Haseltine, A.B. Smith, J. Phys. France **47**, 1533 (1986).
45. T.A. Lobko, B.I. Ostrovskii, W. Haase, J. Phys. II France **2**, 1195 (1992).
46. J. Wang, T.C. Lubensky, J. Phys. France **45**, 1653 (1984).
47. C.R. Safinya, W.A. Varady, L.Y. Chiang, P. Dimon, Phys. Rev. Lett. **57**, 432 (1986).